

Nature Plants

1 **Stimulating photosynthetic processes increases productivity and water use efficiency in**
2 **the field**

3

4 Patricia E. López-Calcano^{1,2*}, Kenny L. Brown^{1,2}, Andrew J. Simkin^{1,2,3}, Stuart J. Fisk²,
5 Silvere Vialet-Chabrand², Tracy Lawson², Christine A. Raines^{2*}

6

7

8 ¹ P.E.L.C, K.L.B. and A.J.S contributed equally to this work

9 ² School of Life Sciences, Wivenhoe Park, University of Essex, Colchester, CO4 3SQ, UK.

10 ³ Genetics, Genomics and Breeding, NIAB EMR New Road, East Malling, Kent, ME19 6BJ.

11 * Address correspondence to C.A.R. (email: rainc@essex.ac.uk) or to P.E.L.C. (email:
12 pelope@essex.ac.uk).

13

14

15 **Short title:** Improving photosynthesis and yield

16 ORCID IDs: 0000-0003-2436-8988 (P.E.L.C); 0000-0002-0587-2698 (K.L.B.); 0000-0001-
17 5056-1306 (A.J.S.); 0000-0002-2105-2825 (S.V.C); 0000-0002-4073-7221 (T.L.); 0000-
18 0001-7997-7823 (C.A.R)

19

20 **One sentence summary:** Simultaneous stimulation of RuBP regeneration and electron
21 transport results in improvements in biomass yield in glasshouse and field grown tobacco.

22

23 **Abstract**

24 Previous studies have demonstrated that independent stimulation of either electron transport
25 or RuBP regeneration can increase the rate of photosynthetic carbon assimilation and plant
26 biomass. In this paper, we present evidence that a multi-gene approach to simultaneously
27 manipulate these two processes provides a further stimulation of photosynthesis. We report
28 on the introduction of the cyanobacterial bifunctional enzyme fructose-1, 6-
29 biphosphatase/sedoheptulose-1,7-bisphosphatase or overexpression of the plant enzyme
30 sedoheptulose-1,7-bisphosphatase, together with expression of the red algal protein
31 cytochrome c_6 , and show that a further increase in biomass accumulation under both
32 glasshouse and field conditions can be achieved. Furthermore, we provide evidence that
33 stimulation of both electron transport and RuBP regeneration can lead to enhanced intrinsic
34 water use efficiency under field conditions.

35

36 **Keywords:** SBPase; FBP/SBPase; Calvin-Benson cycle; cytochrome c_6 ; chlorophyll
37 fluorescence imaging; transgenic; electron transport; biomass; water use efficiency.

38 Yield potential of seed crops grown under optimal management practices, and in the
39 absence of biotic and abiotic stress, is determined by incident solar radiation over the
40 growing season, the efficiency of light interception, energy conversion efficiency and
41 partitioning or harvest index. For the major crops, the only component not close to the
42 theoretical maximum is energy conversion efficiency, which is determined by gross canopy
43 photosynthesis minus respiration. This highlights photosynthesis as a target for improvement
44 to raise yield potential in major seed crops¹⁻³.

45

46 Transgenic experiments and modelling studies have provided compelling evidence
47 that increasing the levels of photosynthetic enzymes in the Calvin Benson (CB) cycle has the
48 potential to impact photosynthetic rate and yield^{1,2,4-15}. Over-expression of SBPase in
49 tobacco^{5,7,8}, Arabidopsis⁹, tomato¹⁵ and wheat¹⁶ has demonstrated the potential of
50 manipulating the expression of CB cycle enzymes and specifically the regeneration of RuBP
51 to increase growth, biomass (30-42%) and even seed yield (10-53%). Similarly,
52 overexpression of other enzymes including FBPA¹⁴, cyanobacterial SBPase, FBPase¹⁷ and
53 the bifunctional fructose-1,6-bisphosphatases/sedoheptulose-1,7-bisphosphatase
54 (FBP/SBPase^{4,18,19}) in a range of species has shown that increasing photosynthesis increases
55 yield. In addition to manipulation of CB cycle genes, increasing photosynthetic electron
56 transport has also been shown to have a beneficial effect on plant growth. Overexpression of
57 the Rieske FeS protein -a key component of the cytochrome *b₆f* complex- in Arabidopsis, has
58 previously been shown to lead to increases in electron transport rates, CO₂ assimilation,
59 biomass and seed yield²⁰. Similar results were also observed when the Rieske FeS protein
60 was over-expressed in the C4 plant *Setaria viridis* demonstrating that this manipulation has
61 the potential to have a positive effect in both C3 and C4 species²¹. Furthermore, the
62 introduction of the algal cytochrome *c₆* protein into Arabidopsis and tobacco resulted in

63 increased growth^{22,23}. In cytochrome *c₆* expressing transgenic plants, the electron transport
64 rate was increased along with ATP, NADPH, chlorophyll, starch content, and capacity for
65 CO₂ assimilation. Higher plants have been proposed to have lost the cytochrome *c₆* protein
66 through evolution, but in green algae and cyanobacteria, which have genes for both
67 cytochrome *c₆* and plastocyanin (PC), cytochrome *c₆* has been shown to replace PC as the
68 electron transporter connecting the cytochrome *b₆f* complex with PSI under Cu deficiency
69 conditions^{24,25}. There is evidence showing that PC can limit electron transfer between
70 cytochrome *b₆f* complex and PSI²⁶, and in Arabidopsis, it has been shown that introduced
71 algal cytochrome *c₆* is a more efficient electron donor to P700 than PC²². This evidence
72 suggests the introduction of the cytochrome *c₆* protein in higher plants as a viable strategy for
73 improving photosynthesis.

74 This paper aims to test the hypothesis that combining an increase in the activity of a
75 CB cycle enzyme, specifically enhancing RuBP regeneration, together with stimulation of the
76 electron transport chain can boost photosynthesis and yield above that observed when these
77 processes are targeted individually. *Nicotiana tabacum* plants expressing the cyanobacterial
78 FBP/SBPase or the higher plant SBPase, and the algal cytochrome *c₆* were generated using
79 two different tobacco cultivars. The analysis presented here demonstrates that the
80 simultaneous stimulation of electron transport and RuBP regeneration leads to a significant
81 increase in photosynthetic carbon assimilation, and results in increased biomass and yield
82 under both glasshouse and field conditions.

83

84 **Production and Selection of Tobacco Transformants**

85 Previous differences observed in the biomass accumulation between Arabidopsis and
86 tobacco overexpressing SBPase and SBPase plus FBPA^{8,9} led us to explore the effect of
87 similar manipulations (RuBP regeneration by overexpression of SBPase or introduction of
88 the cyanobacterial FBP/SBPase, together with enhanced electron transport) in two different
89 tobacco cultivars with different growth habits: *N. tabacum* cv. Petite Havana, with
90 indeterminate growth, and *N. tabacum* cv. Samsun, with determinate growth. Sixty lines of
91 cv. Petit Havana, and up to fourteen lines of cv. Samsun were generated per construct and T0
92 and T1 transgenic tobacco were screened by qPCR and immuno-blot analysis to select
93 independent lines with expression of the transgenes (data not shown).

94 *N. tabacum* cv. Petit Havana T2/T3 progeny expressing FBP/SBPase (S_B ; lines S_{B03} ,
95 S_{B06} , S_{B21} , S_{B44}) or cytochrome c_6 (C_6 ; lines C15, C41, C47, C50) and cv. Samsun lines
96 expressing SBPase + cytochrome c_6 (SC_6 , lines SC1, SC2 and SC3) were produced by
97 agrobacterium transformation. *N. tabacum* cv. Petit Havana plants expressing both S_B and C_6
98 were generated by crossing S_B lines (S_{B06} , S_{B21} , S_{B44}) with C_6 lines (C15, C47, C50) to
99 generate four independent $S_B C_6$ lines: S_{BC1} (S_{B06} x C47), S_{BC2} (S_{B06} x C50), S_{BC3} (S_{B44} x
100 C47) and S_{BC6} (S_{B21} x C15). Semi-quantitative RT-PCR was used to detect the presence of
101 the FBP/SBPase transcript in lines S_B and $S_B C_6$, cytochrome c_6 in lines C_6 , $S_B C_6$ and SC_6 , and
102 SBPase in lines S and SC_6 (**Supplementary Fig. 1**). The selected S_B and $S_B C_6$ lines were
103 shown to accumulate FBP/SBPase protein, and S and SC_6 to overexpress the SBPase protein
104 by immunoblot analysis (**Fig. 1a and Supplementary Fig. 2**). In addition to immunoblot
105 analysis, we analysed total extractable FBPase activity in the leaves of the cv. Petite Havana
106 T2/T3 & F3 homozygous progeny lines used to determine chlorophyll fluorescence and
107 photosynthetic parameters. This analysis showed that these plants (S_B and $S_B C_6$) had
108 increased levels of FBPase activity ranging from 34 to 47% more than the control plants (**Fig.**

109 **1c)**. The full set of assays showing the variation in FBPase activities between plants can be
110 seen in supplemental data (**Supplementary Fig. 3**). The S and SC₆ lines were from the same
111 generation of transgenic plants used in a previous study and shown to have increased SBPase
112 activity⁸. The cytochrome *c*₆ antibody (raised against a peptide from the *Porphyra umbilicalis*
113 protein) was unable to detect less than 60 ng of purified cytochrome *c*₆ protein extracted from
114 *E. coli* (**Supplementary Fig. 4**), and immunoblotting of leaf extracts did not result in a
115 signal. However, when semi-purified extracts from lines C15, C41 and C47 were used, a
116 band of the expected molecular weight was identified in semi-purified extracts from lines
117 C15, C41 and C47, providing qualitative confirmation of the presence of cytc₆ in the
118 transgenic tobacco plants (**Fig. 1b and Supplementary Fig. 5a**). No bands were observed in
119 semi-purified extracts from control (CN) plants. To provide further evidence of the presence
120 of introduced cytochrome *c*₆ protein a spectral scan was run using the semi-purified protein
121 extracts of C₆ and CN plants; the solet peak at 420 nm demonstrated the presence of the heme
122 group and was only detectable in the C₆ transgenic plants and not in the CN plants.
123 (**Supplementary Fig. 5b**). Additionally, a physiological assay probing the response of
124 photosynthesis during light induction was performed. CN and C₆ plants were provided with
125 saturating light and [CO₂] following a period of darkness. The C₆ plants were shown to have
126 both a more rapid response and greater rate of net CO₂ assimilation compared with CN plants
127 (**Supplementary Fig. 6a & 6d**). The faster increase in *A* was accompanied by a quicker rise
128 in the operating efficiency of both PSII (F_q'/F_m') and PSI (YI) providing evidence that in
129 these plants electron flow through both photosystems was increased. This increase in electron
130 transport could contribute to the higher *A* rates observed by providing the required energy
131 (ATP) and reductant (NADPH). This response was further accelerated in S_BC₆ transgenic
132 plants mostly likely due to the increased sink capacity provided by CB cycle activity
133 (**Supplementary Fig. 6**).

134

135 Chlorophyll fluorescence analysis confirmed that in young plants, the operating
136 efficiency of photosystem two (PSII) photochemistry F_q'/F_m' at an irradiance of 600-650
137 $\mu\text{mol m}^{-2} \text{s}^{-1}$ was significantly higher in all selected lines compared to either WT or null
138 segregant controls (**Fig. 1d, e**). However, the F_q'/F_m' values of the $S_B C_6$ and SC_6 lines, were
139 not significantly different from the F_q'/F_m' values obtained from the plants expressing
140 individually FBP/SBPase (S_B), cytochrome c_6 (C_6) or SBPase (S).

141

142 **Stimulation of electron transport and RuBP regeneration increases photosynthesis**

143 Transgenic lines selected based on the initial screens described above were grown in
144 the glasshouse, in natural light supplemented to provide illumination between 400-1000 μmol
145 $\text{m}^{-2} \text{s}^{-1}$. The rate of net CO_2 assimilation (A) and F_q'/F_m' was determined as a function of
146 internal CO_2 concentration (C_i), in mature and developing leaves of *N. tabacum* cv. Samsun
147 (S and SC_6) and in mature leaves of *N. tabacum* cv. Petit Havana (S_B , C_6 and $S_B C_6$) (**Fig. 2**).
148 The transgenic plants displayed greater CO_2 assimilation rates than those of the control (CN)
149 plants. A was 15% higher than the controls in the mature leaves of the SC_6 , at a C_i of
150 approximately 300 $\mu\text{mol mol}^{-1}$ (the C_i prevailing at current atmospheric [CO_2]) (**Fig. 2b**). The
151 developing leaves of the SC_6 plants also showed significant increases in PSII operating
152 efficiency (F_q'/F_m') and in the PSII efficiency factor (F_q'/F_v' ; which is determined by the
153 ability of the photosynthetic apparatus to maintain Q_A in the oxidized state and therefore a
154 measure of photochemical quenching) when compared to control plants (**Fig. 2c**).
155 Interestingly, in mature leaves of the cv. Samsun transgenic plants, the differences in
156 assimilation rates and in the operating efficiency of PSII photochemistry between the
157 transgenic and the CN plants were smaller than in the developing leaves. Only the S
158 transgenic plants displayed a higher average value for F_q'/F_m' and F_q'/F_v' than the CN plants

159 at all CO₂ concentrations measured. In contrast, the mature leaves of SC₆ plants displayed
160 F_q'/F_v' values higher than the control only at C_i levels between 300 and 900 μmol mol⁻¹ (**Fig.**
161 **2b**).

162 Similar trends were shown for the *N. tabacum* cv. Petit Havana transgenic plants,
163 which displayed higher average values of A and F_q'/F_m' than the CN (**Fig. 2a**). In the leaves
164 of the S_BC₆ plants (cv. Petit Havana) these significant increases were similar to the
165 developing leaves of the SC₆ lines (cv. Samsun). No significant differences in PSII maximum
166 efficiency (F_v'/F_m') were observed between the CN and the transgenics in either cultivar.

167 The developing leaves of both the S and SC₆ plants (cv. Samsun) showed a
168 significant increase in both the maximum electron transport and RuBP regeneration rate
169 (J_{max}) and maximum assimilation (A_{max}) when compared the control plants (**Table 1**). The
170 mature leaves of the SC₆ (cv. Samsun) and S_BC₆ (cv. Petite Havana) transgenics also
171 displayed a significantly higher A_{max} than the CN, and higher average values for $V_{C_{max}}$, and
172 J_{max} were also evident in these leaves. These results showed that simultaneous stimulation of
173 electron transport and RuBP regeneration by expression of cytochrome c_6 in combination
174 with FBP/SBPase or SBPase has a greater impact on photosynthesis than the single
175 manipulations in all plants analysed.

176

177 **Stimulation of electron transport and RuBP regeneration improves growth**

178 In parallel experiments, plants expressing FBP/SBPase (S_B), cytochrome c_6 (C₆) and
179 both (S_BC₆) (*N. tabacum* cv. Petite Havana) and plants expressing SBPase (S) and SBPase +
180 cytochrome c_6 (SC₆) (*N. tabacum* cv. Samsun) were grown in the glasshouse for four and six
181 weeks respectively before harvesting. Height, leaf number, total leaf area and above ground
182 biomass were determined (**Fig 3** and **Supplementary Fig 7**). All of the transgenic plants
183 analysed here displayed increased height when compared to CN plants. Plants expressing

184 cytochrome c_6 (C_6 , $S_B C_6$, (cv. Petite Havana) and SC_6 (cv. Samsun)) had a significant increase
185 in leaf area and in stem and leaf biomass compared to their respective controls (**Fig.3** and
186 **Supplementary Fig. 8,9**). In the S_B transgenic plants (cv. Petite Havana) only the biomass of
187 the stem was greater than the CN plants. Notably the $S_B C_6$ and SC_6 transgenics displayed
188 significantly greater leaf area than the single S_B and S transgenic plants respectively. The
189 total increase in above ground biomass when compared to CN group was 35% in S_B , 44% in
190 C_6 and 9% in S , with consistently higher means in the double manipulations $S_B C_6$ (52%) and
191 SC_6 (32%) (**Fig.3**).

192

193 **Expression of FBP/SBPase and cytochrome c_6 increases growth and water use efficiency**

194 To test whether the increases in biomass observed in these transgenic plants under
195 glasshouse conditions could be reproduced in a field environment, a subset of lines was
196 selected for testing in the field. Since the larger percentage increases in biomass were
197 displayed by the manipulations in *N. tabacum* cv. Petit Havana, these plants were selected
198 and tested in three field experiments in two different years (2016 and 2017).

199 In 2016, a small-scale replicated control experiment was carried out to evaluate
200 vegetative growth in the field, in the lines expressing single gene constructs for FBP/SBPase
201 (S_B) and cytochrome c_6 (C_6) (**Supplementary Fig. 14a**). Plants were germinated and grown
202 under controlled environment conditions for 25 d before being moved to the field. After 14 d
203 in the field, plants were harvested at an early vegetative stage and plant height, total leaf area
204 and above ground biomass were measured (**Fig. 4 (a-c)** and **Supplementary Fig. 10a**). These
205 data revealed that the S_B and C_6 plants showed an increase in height, leaf area and above
206 ground biomass of 27%, 35% and 25% respectively for S_B and 50%, 41% and 36%
207 respectively for C_6 when compared to CN plants.

208 In 2017, two larger scale, randomized block design field experiments were carried out
209 to evaluate performance in the S_B , C_6 and $S_B C_6$ plants compared to CN plants
210 (**Supplementary Fig.14b**). Plants were grown from seed in the glasshouse for 33 d, and then
211 moved to the field and allowed to grow until the onset of flowering (further 24-33 d), before
212 harvesting. In **Fig. 4d-i** it can be seen that the S_B and C_6 plants harvested after the onset of
213 flowering did not display any significant increases in height, leaf area or biomass when
214 compared to CN plants. Interestingly, plants expressing both FBP/SBPase and cytochrome c_6
215 ($S_B C_6$), displayed a significant increase in a number of growth parameters; with 13%, 17%
216 and 27% increases in height, leaf area and above ground biomass respectively when
217 compared to CN plants.

218 Additionally, in the 2017 field experiments A as a function of C_i at saturating light
219 (A/C_i) was determined. In the 2017 Experiment 1 a significant increase in A was observed in
220 S_B and C_6 plants without differences in PSII operating efficiency (F_q'/F_m') (**Fig. 5a**).
221 However, in the 2017 Experiment 2, no differences in A or in F_q'/F_m' values were evident in
222 the C_6 and $S_B C_6$ plants when compared to the CN plants (**Fig. 5b**). Analysis of A as a function
223 of light (A/Q) showed either small or no significant differences in A between genotypes (**Fig.**
224 **6a** and **Supplementary Fig 11a**). Interestingly, g_s in the $S_B C_6$ plants was significantly lower
225 than for the C_6 and CN plants at light intensities above $1000 \mu\text{mol m}^{-2} \text{s}^{-1}$ (**Fig 6b**), resulting
226 in a significant increase in intrinsic water use efficiency ($iWUE$) for $S_B C_6$ plants (**Fig 6d**). No
227 significant differences in $iWUE$ were observed for S_B or C_6 transgenic plants (**Fig 6d** and
228 **Supplementary Fig 11d**).

229 **DISCUSSION**

230 In this study, we describe the generation and analysis of transgenic plants with
231 simultaneous increases in electron transport and improved capacity for RuBP regeneration, in
232 two different tobacco cultivars. Here we have shown that independent stimulation of electron
233 transport (by expression of cytochrome c_6) and stimulation of RuBP regeneration (by
234 expression of FBP/SBPase or overexpression of SBPase) increased photosynthesis and
235 biomass in glasshouse studies. Furthermore, we demonstrated how the targeting of these two
236 processes simultaneously (in the $S_B C_6$ and SC_6 plants) had an even greater effect in
237 stimulating photosynthesis and growth. Additionally, in field studies we demonstrate that
238 plants with simultaneous stimulation of electron transport and of RuBP regeneration had
239 increased *iWUE* with an increase in biomass.

240

241 Under glasshouse conditions, increases in photosynthesis were observed in all of the
242 transgenic plants analysed here and this was found to be correlated with increased biomass.
243 Although increases in photosynthesis and biomass have been reported for plants with
244 stimulation of RuBP regeneration in both model^{4,5,8,7,27} and crop^{18,16} species; and electron
245 transport in Arabidopsis and tobacco^{20,22,28}, the data presented here provides the first report of
246 increased photosynthesis and biomass by the simultaneous stimulation of electron transport
247 and RuBP regeneration. Increases in A were observed under glasshouse conditions in the
248 leaves of all of the different transgenic tobacco plants and in both tobacco cultivars (cv. Petit
249 Havana and cv. Samsun). Analysis of the A/C_i response curves showed that the average
250 values for the photosynthetic parameters $V_{C_{max}}$, J_{max} and A_{max} increased by up to 11, 14 and
251 15% respectively. These results indicated that not only was the maximal rate of electron
252 transport and RuBP regeneration increased, but the rate of carboxylation by Rubisco was also
253 increased. Although this may seem counterintuitive in that we have not targeted directly

254 Rubisco activity, it is in keeping with a study by Wullschleger²⁹ of over 100 plant species that
255 showed a linear correlation between J_{\max} and $V_{C_{\max}}$. Furthermore, it has also been shown
256 previously that overexpression of SBPase leads not only to a significant increase in J_{\max} but
257 that an increase in $V_{C_{\max}}$ and Rubisco activation state^{5,8}.

258

259 Notably, in the greenhouse study, the highest photosynthetic rates were observed in plants
260 in which both electron transport and RuBP regeneration ($S_B C_6$ and SC_6) were boosted,
261 suggesting that the co-expression of these genes results in an additive effect on improving
262 photosynthesis. In addition to the increases in A , the plants with simultaneous stimulation of
263 electron transport and RuBP regeneration displayed a significant increase in F_q'/F_m' ,
264 indicating a higher quantum yield of linear electron flux through PSII compared to the control
265 plants. These results are in keeping with the published data for the introduction of
266 cytochrome c_6 and the overexpression of the Rieske FeS protein in Arabidopsis^{20,22}. In these
267 studies the plants had a higher quantum yield of PSII and a more oxidised plastoquinone
268 pool²², suggesting that, although PC is not always limiting under all growth conditions³⁰,
269 there is scope to stimulate reduction of PSI by using alternative, more efficient electron
270 donors to PSI like cytochrome c_6 ^{22,26}. Furthermore, in the $S_B C_6$ and SC_6 plants the increase in
271 F_q'/F_m' was found to be largely driven by the increase in the PSII efficiency factor (F_q'/F_v').
272 This suggests that the increase in efficiency in these plants is likely due to stimulation of
273 processes down stream of PSII such as CO₂ assimilation.

274

275 To provide further evidence of the applicability of targeting both electron transport and
276 RuBP regeneration to improve crop yields, we tested these plants in the field. Here we
277 showed that the expression FBP/SBPase alone led to an increase in growth and biomass in
278 the 2016 field-grown plants of between 22-40%, when harvested during early vegetative

279 growth, prior to the onset of flowering. Interestingly, when these plants were harvested later in
280 development, after the onset of flowering, in the 2017 field trials, this advantage was no
281 longer evident and the single FBP/SBPase expressors were indistinguishable from the control
282 plants. These results are in contrast to the 2016 field data and may be due to the later timing
283 in development of the harvest in the 2017 experiment. The transgenic plants expressing
284 cytochrome c_6 alone also showed enhanced growth and biomass early development, but as
285 with the FBPase/SBPase plants, this improvement was no longer evident when plants were
286 harvested after flowering. This difference in biomass gain between the early and late harvest
287 was not observed in a parallel experiment, where the overexpression of H-protein was shown
288 to increase biomass under field conditions in plants harvested in early development and after
289 the onset of flowering³¹. These results suggest that the expression of FBP/SBPase or
290 cytochrome c_6 alone, may provide an advantage under particular sets of conditions or at
291 specific stages of plant development. This might be exploitable for some crops where an
292 early harvest is desirable (eg. some types of lettuce, spinach and tender greens)¹⁸. In contrast
293 to the results with the single manipulations described above, plants expressing both
294 cytochrome c_6 and FBP/SBPase simultaneously displayed a consistent increase in biomass
295 after flowering under field conditions.

296

297 In the transgenic lines grown in the field, the correlation between increases in
298 photosynthesis and increased biomass were less consistent than that observed under
299 glasshouse conditions. The significant increases in photosynthetic capacity displayed by the
300 FBP/SBPase and cytochrome c_6 expressors in 2017 Experiment 1, provided clear evidence
301 that these individual manipulations are able to significantly stimulate photosynthetic
302 performance under field conditions. However, no increase in biomass was evident in these
303 plants. In contrast, in the 2017 Experiment 2 we did not detect any significant differences in

304 photosynthetic capacity in either the cytochrome c_6 expressors or the plants with
305 simultaneous expression of FBP/SBPase + cytochrome c_6 expressors, but increased biomass
306 was evident. At this point we have no explanation for this disparity. However, although not
307 significantly different, in all experiments, the mean A values of the transgenic plants were
308 consistently higher than those of the controls. It is known that even small increases in
309 assimilation throughout the lifetime of a plant will have a cumulative effect, which could
310 translate into a significant biomass accumulation⁸, this may in part explain the disparity with
311 the biomass results presented. Furthermore, the phenotyping experiments carried out on C_6
312 and $S_B C_6$ plants (**Supplementary Fig 6**) showed that there was a more rapid induction of
313 photosynthesis, particularly in $S_B C_6$ plants. This characteristic might also contribute to an
314 increase in photosynthetic rates and biomass when plants are grown in fluctuating light
315 conditions, but would not be detectable in the steady-state measurements performed in our
316 field experiments.

317

318

319 An unexpected result that was found in the plants with simultaneous expression of
320 FBP/SBPase + cytochrome c_6 ($S_B C_6$), is that these plants had a lower g_s and lower C_i at light
321 intensities above $1000 \mu\text{mol m}^{-2} \text{s}^{-1}$, when compared to control plants. Normally, lower C_i
322 would be expected to lead to a reduction in photosynthesis, but the $S_B C_6$ plants were able to
323 maintain CO_2 assimilation rates equal to or higher than control plants resulting in an
324 improvement in $iWUE$. A similar improvement in $iWUE$ was seen in plants overexpressing
325 the NPQ related protein, PsbS³². It was shown that light-induced stomatal opening was
326 reduced in these plants in which a more oxidized Q_A pool was found and this has been
327 proposed to act as a signal in stomatal movement³³. This higher $iWUE$ and the fact that a
328 higher productivity than controls has been reported in field studies for transgenic lines with

Nature Plants

329 increased RuBP regeneration grown under CO₂ enrichment^{7,18}, highlight the potential of
330 manipulating electron transport and RuBP regeneration in the development of new varieties
331 able to sustain photosynthesis and yields under climate change scenarios.

332 **MATERIALS AND METHODS**

333

334 **Generation of constructs and transgenic plants**

335 Constructs were generated using Golden Gate cloning^{34,35} or Gateway cloning
336 technology³⁶. Transgenes were under the control of CaMV35S and FMV constitutive
337 promoters. Construct detail below and in **Supplementary Fig. 12**.

338 For *N. tabacum* cv. Petit Havana, the codon optimised cyanobacterial bifunctional
339 fructose-1,6-bisphosphatases/sedoheptulose-1,7-bisphosphatase (FBP/SBPase; *slr2094*
340 *Synechocystis* sp. PCC 7942⁴ linked to the geraniol synthase transit peptide³⁷ and the codon
341 optimised *P. umbilicalis*'s cytochrome *c*₆ (AFC39870) with the chlorophyll a-b binding
342 protein 6 transit peptide from Arabidopsis (AT3G54890) were used to generate Golden
343 Gate³⁵ over-expression constructs (EC23083 and EC23028) driven by the FMV³⁸ and CaMV
344 35S promoters respectively (**Supplementary Fig. 12a**).

345 The cytochrome *c*₆ from *P. umbilicalis* was selected as it is commonly found on the
346 UK coastline and it shares over 86% identity with previously published *P. yeoensis* and *Ulva*
347 *fasciata* used by Chida *et al*²² and Yadav *et al*²³. The level of similarity between these
348 proteins and the fact that the functional regions are identical, provides confidence that the
349 cytochrome *c*₆ proteins from these three species function in a similar way (see alignment in
350 **Supplementary Fig. 13**). The *P. umbilicalis* cytochrome *c*₆ was linked to the transit peptide
351 from the light-harvesting complex I chlorophyll a/b binding protein 6 (At3g54890) to
352 generate an over-expression construct driven by the CaMV 35S promoter; B2-C6 in the
353 vector pGWB2³⁶ used for *N. tabacum* cv. Samsun transformation (**Supplementary Fig. 12b**).
354 The recombinant plasmid B2-C6, was introduced into SBPase over-expressing tobacco cv.
355 Samsun⁵ using *Agrobacterium tumefaciens* AGL1 via leaf-disc transformation³⁹. Primary
356 transformants (39) (T0 generation) were regenerated on MS medium containing kanamycin

Nature Plants

357 (100 mg L⁻¹), hygromycin (30 mg L⁻¹) and augmentin (500 mg L⁻¹). Plants expressing the
358 integrated transgenes were screened using RT-PCR (data not shown).

359 Similarly, the recombinant plasmids EC23083, and EC23028 were introduced into
360 wild type tobacco (*Nicotiana tabacum*) cv Petit Havana, using *A. tumefaciens* strain
361 LBA4404 via leaf-disc transformation³⁹, and shoots regenerated on MS medium containing,
362 hygromycin (20 mg L⁻¹) and cefotaxime (400 mg L⁻¹). Hygromycin resistant primary
363 transformants (T0 generation) with established root systems were transferred to soil and
364 allowed to self-fertilize.

365 Between twelve and 60 independent lines were generated per construct and 3-4 lines
366 taken forward for further analysis. Control (CN) plants used in this study were a combination
367 of WT and null segregant plants from the transgenic lines, verified by PCR for non-
368 integration of the transgene.

369

370 **Plant Growth**

371 *Controlled conditions*

372 Wild-type tobacco plants and T1 progeny resulting from self-fertilization of
373 transgenic plants were grown to seed in soil (Levington F2, Fisons, Ipswich, UK). Lines of
374 interest were identified by immunoblot and qPCR. For the experiments in the Samsun cv. the
375 null segregants were selected from transformed lines. For Petit Havana, the null segregants
376 were selected from the S_BC₆ lines. For experimental study, T2-T4 and F1-F3 progeny seeds
377 were germinated on soil in controlled environment chambers at an irradiance of 130 μmol
378 photons m⁻² s⁻¹, 22°C, relative humidity of 60%, in a 16-h photoperiod. Plants were
379 transferred to individual 8 cm pots and grown for two weeks at 130 μmol photons m⁻² s⁻¹,
380 22°C, relative humidity of 60%, in a 16-h photoperiod. Plants were transferred to 4 L pots
381 and cultivated in a controlled environment glasshouse (16-h photoperiod, 25°C-30°C

Nature Plants

382 day/20°C night, and natural light supplemented under low light induced by cloud cover with
383 high-pressure sodium light bulbs, giving 380-1000 $\mu\text{mol m}^{-2} \text{s}^{-1}$ (high-light) from the pot
384 level to the top of the plant, respectively). Positions of the plants were changed 3 times a
385 week and watered regularly with a nutrient medium⁴⁰. Plants were positioned such that at
386 maturity, a near-to-closed canopy was achieved and the temperature range was maintained
387 similar to the ambient external environment. Four leaf discs (0.8 cm diameter) were taken for
388 immunoblot analysis and FBPase activity. These disks were taken from the same areas of the
389 leaf used for photosynthetic measurements, immediately plunged into liquid N₂ and stored at
390 -80°C.

391

392 *Field studies*

393 Plants were grown as described in Lopez-Calcano et al³¹, and with a methodology
394 broadly analogous to that used commercially for this crop. The field site was situated at the
395 University of Illinois Energy Farm (40.11°N, 88.21°W, Urbana, IL). Two different
396 experimental designs were used in 2 different years.

397 2016: Replicated control design (**Supplementary Fig. 14a**). Plants were grown in
398 rows, spaced 30 cm apart with the outer boundary being a wild-type border. The entire
399 experiment was surrounded by two rows of wild-type borders. Plants were irrigated when
400 required using rain towers. T2 seed was germinated and after 11 d were moved to individual
401 pots (350 mL). The seedlings were grown in the glasshouse for further 15 d before being
402 moved into the field, and allowed to grow in the field for 14 d before harvest.

403 2017: Two experiments were carried out two weeks apart. A blocks-within-rows
404 design was used (**Supplementary Fig. 14b**) where 1 block holds one line of each of the five
405 manipulations and each row has all lines. The central 20 plants of each block are divided into
406 five rows of four plants per genotype. The 2017 Exp.1 contained controls (WT and null

407 segregants), FBP/SBPase expressing lines (S_B) and cytochrome c_6 expressing lines (C_6). The
408 2017 Exp. 2 contained controls (WT and null segregants), cytochrome c_6 expressing lines
409 (C_6), and FBP/SBPase + cytochrome c_6 expressing lines ($S_B C_6$). Seed was germinated and
410 after 12 d moved to hydroponic trays (Trans-plant Tray GP009 6912 cells; Speedling Inc.,
411 Ruskin, FL), and grown in the glasshouse for 20 d before being moved to the field. The plants
412 were allowed to grow in the field until flowering (approximately 30 d) before harvest.

413 The field was prepared in a similar fashion each year as described in Kromdijk *et al*⁴¹.
414 Light intensity (LI-quantum sensor; LI-COR) and air temperature (Model 109 temperature
415 probe; Campbell Scientific Inc, Logan, UT) were measured nearby on the same field site, and
416 half-hourly averages were logged using a data logger (CR1000; Campbell Scientific).

417

418 **cDNA generation and RT-PCR**

419 Total RNA was extracted from tobacco leaf disks (sampled from glasshouse grown
420 plants and quickly frozen in liquid nitrogen) using the NucleoSpin® RNA Plant Kit
421 (Macherey-Nagel, Fisher Scientific, UK). cDNA was synthesized using 1 μg total RNA in 20
422 μl using the oligo-dT primer according to the protocol in the RevertAid Reverse
423 Transcriptase kit (Fermentas, Life Sciences, UK). cDNA was diluted 1 in 4 to a final
424 concentration of 12.5 $\text{ng } \mu\text{L}^{-1}$. For semi quantitative RT-PCR, 2 μL of RT reaction mixture
425 (100 ng of RNA) in a total volume of 25 μL was used with DreamTaq DNA Polymerase
426 (Thermo Fisher Scientific, UK) according to manufacturer's recommendations. PCR products
427 were fractionated on 1.0% agarose gels. For qPCR, the SensiFAST SYBR No-ROX Kit was
428 used according to manufacturer's recommendations (Bioline Reagents Ltd., London, UK).
429 Primers used for semi quantitative RT-PCR can be seen in **Supplementary Table 1**.

430

431 **Protein Extraction and immunoblot analysis**

432 Leaf discs sampled as described above, or fresh *Porphyra umbilicalis* samples, were
433 ground in dry ice and protein extractions performed as described in Lopez-Calcano *et al.*⁴²,
434 or using the nucleospin RNA/Protein kit (Macherey-Nagel (<http://www.mn-net.com/>) during
435 RNA preparations. Protein quantification was performed using the protein quantification Kit
436 from Macherey-Nagel. Samples were loaded on an equal protein basis, separated using 12%
437 (w/v) SDS-PAGE, transferred to a nitrocellulose membrane (GE Healthcare Life science,
438 Germany), and probed using antibodies raised against SBPase and FBP/SBPase. Proteins
439 were detected using horseradish peroxidase conjugated to the secondary antibody and ECL
440 chemiluminescence detection reagent (Amersham, Buckinghamshire, UK). SBPase
441 antibodies are previously characterised^{5,43}. FBP/SBPase antibodies were raised against a
442 peptide from a conserved region of the protein [C]-DRPRHKELIQEIRNAG-amide, and
443 cytochrome *c*₆ antibodies were raised against peptide [C]-[Nle]-PDKTLKKDVLEANS-
444 amide (Cambridge Research Biochemicals, Cleveland, UK). In addition to the
445 aforementioned antibodies, samples were probed using antibodies raised against
446 transketolase^{44,45} as loading controls.

447

448 **Protein Extraction from plants for cytochrome *c*₆ analysis.**

449 Whole leaves were harvested from 8 week old plants, washed in cold water and then
450 wiped with a cloth soaked in 80 % ethanol to remove the majority of leaf residue. The leaves
451 were then washed twice more in cold water, the mid rib was removed and 50 g of the
452 remaining tissue was placed in a sealed plastic bag and stored overnight in the dark at 4°C.
453 Proteins were extracted as in Hiyama⁴⁷, with a few modifications. Leaf tissue was
454 homogenised in 250 ml of chilled chloroplast preparation buffer (50 mM sodium phosphate
455 buffer, pH 7, 10 mM NaCl) for 30 seconds. The solution was then filtered through 4 layers of
456 muslin cloth and centrifuged at 10,000 g for 5 minutes. The resulting pellet was then gently

457 resuspended in 50 ml of chilled chloroplast preparation buffer and the chlorophyll
458 concentration was measured and adjusted to approximately 2 mg ml⁻¹. The resultant mixture
459 was then added to two volumes of preheated (45°C) solubilisation medium (50 mM Tris-HCl
460 pH 8.8 and 3% triton X) and incubated at 45°C for 30 minutes and then chilled in an ice bath
461 for a further 30 minutes before centrifugation at 12000 g for 30 minutes. The supernatant was
462 stored at -80°C for use in the next stage. To purify cytochrome *c*₆ protein a Biorad Econo-Pac
463 High-Q, 5 ml type wash column was used at a flow rate of 1 ml min⁻¹. First the column was
464 prepared by washing it with 100 ml of starting buffer (Starting buffer: 10 mM Tris-HCl pH
465 8.8, 0.2% triton X 100 and 20% sucrose). Then the protein mixture from the previous step
466 was diluted with an equal volume of chilled starting buffer and passed through the column at
467 a flow rate of 1 ml min⁻¹. Once all the protein was loaded onto the column it was then washed
468 with 1000 ml of starting buffer supplemented with 10 mM NaCl. Then 300 ml of starting
469 buffer supplemented with 50 ml NaCl and finally a linear gradient of starting buffer from 50
470 to 200 mM NaCl over a period of 4 hours at 1 ml min⁻¹ was performed and aliquots were
471 collected. For immunoblotting, samples were acetone precipitated and the dried protein pellet
472 then resuspended in 400 µl of solubilisation buffer (7 M urea, 2 M thiourea, 50 mM DTT, 4
473 % CHAPS, 0.4 % SDS, 5 mM K₂CO₃), finally 300 µl loading buffer was added (50%
474 glycerol, 25% β-mecaptoethanol, 25% EDTA) and the samples heated at 90°C for 10 minutes
475 before being loaded on an equal protein basis. Proteins were separated using 18% (w/v) SDS-
476 PAGE, transferred to nitrocellulose membrane, and probed using antibodies raised against a
477 cytochrome *c*₆ peptide. For identification of soret peak, instead of acetone precipitation,
478 extracts were concentrated by spinning at 8,000 g and 4°C over night, using a Vivaspin 20
479 column (GE 28-9323-59), and a spectral scan was done in a SPECTROstar Omega plate
480 reader from BMG Labtech.

481

482 **Recombinant cytochrome c_6 protein production in *E. coli* and purification**

483 pEC86 (CCOS Accession: CCOS891) containing *E. coli* cells were transformed with
484 a pET28b plasmid containing the sequence for the mature cytochrome c_6 and grown in
485 kanamycin (50 ug/ml) and chloramphenicol (35ug/ml) containing LB media. IPTG (119 μ g
486 ml^{-1}) was added to the culture when OD_{600} reached 0.5-0.6. Five hours later 330 $\mu\text{l L}^{-1}$ of 1 M
487 ferriprotoporphyrin IX chloride was added to the media and 24 hours post IPTG, an metal ion
488 master mix (2 mM Ni^{2+} , 2 mM Co^{2+} , 10mM Zn^{2+} , 10 mM Mn^{2+} and 50 mM Fe^{3+}) was added
489 (1.5 ml L^{-1}). Cells were harvested after 5 days of growth and stored at -20 °C. Pellet from 500
490 ml was resuspended in 3 ml of lysis buffer (50mM Tris HCl pH 7.5, 1mM DTT, 1mM
491 PMSF), sonicated (11 cycles of 30 sec sonication 30 sec rest, at 4°C) and then spun twice at
492 10000 g for 20 min at 4 °C. The supernatant was collected and 2 ml loaded in a 124 ml GE
493 Hi Load 16/400 Superdex 75 pg (size exclusion) column. Protein was eluted with 0.05 M
494 Na_2PO_4 pH 7.2, 0.5 M NaCl buffer, at a 1 ml min^{-1} speed and samples were collected every 5
495 ml. Fractions collected between 80-100 min were concentrated by spinning them at 8000 g
496 over night at 4 °C using a Vivaspin 20, (GE 28-9323-59) column. Protein concentration was
497 determined using Bradford quantification, serial dilutions done with 50 mM Tris HCl pH 7.5
498 buffer and spectral scans done in a SPECTROstar Omega plate reader from BMG Labtech as
499 with the semi-purified plant cytochrome c_6 samples.

500

501 **Determination of FBPase and Transketolase Activities**

502 FBPase activity was determined by phosphate release as described previously for
503 SBPase with minor modifications⁸. Leaf discs were isolated from the same leaves and frozen
504 in liquid nitrogen after photosynthesis measurements were completed. Leaf discs were
505 ground to a fine powder in liquid nitrogen and immersed in extraction buffer (50 mM
506 HEPES, pH8.2; 5 mM MgCl ; 1 mM EDTA; 1 mM EGTA; 10% glycerol; 0.1% Triton X-

507 100; 2 mM benzamidine; 2 mM aminocaproic acid; 0.5 mM phenylmethylsulfonylfluoride;
508 10 mM dithiothreitol), centrifuged 1 min at 14,000 g, 4°C. The resulting supernatant (1 ml)
509 was desalted through an NAP-10 column (Amersham) and stored in liquid nitrogen. The
510 assay was carried out as described in Simkin *et al.*⁸. In brief, 20 µl of extract was added to 80
511 µl of assay buffer (50 mM Tris, pH 8.2; 15 mM MgCl₂; 1.5 mM EDTA; 10 mM DTT; 7.5
512 mM fructose-1,6-bisphosphate) and incubated at 25 °C for 30 min. The reaction was stopped
513 by the addition of 50 µl of 1 M perchloric acid. 30 µl of samples or standards (PO₄³⁻ 0.125 to
514 4 nmol) were incubated 30 min at room temperature following the addition of 300 µl of
515 Biomol Green (Affiniti Research Products, Exeter, UK) and the A620 was measured using a
516 microplate reader (VERSAmax, Molecular Devices, Sunnyvale, CA). Activities were
517 normalized to transketolase activity⁴⁸. For transketolase activity assays 230 µl of pre-
518 prepared assay mix comprising of: 14.4 Mm ribose-5-phosphate, 190 µM NADH, 380 µM
519 TPP, 250 U L⁻¹ glycerol-3 phosphate dehydrogenase (G3PDH) and 6500 U L⁻¹ triose
520 phosphate isomerase was transferred to a 96 well plate (Greiner Bio-One) and placed in a
521 plate reader which was set at 23 °C for 5 minutes to stabilise. The plate was then ejected and
522 20 µl of each protein sample used for FBPase activity was injected into the wells containing
523 the assay mix. The plate was then read for absorbance at 340 nm every 5 min for 1 hr.
524 Activity levels were estimated by subtracting the absorbance value when the reaction
525 becomes linear from the absorbance value 20 to 30 minutes after the first absorbance reading
526 depending on the rate of the reaction.

527

528 **Chlorophyll fluorescence imaging screening in seedlings**

529 Chlorophyll fluorescence imaging was performed on 2-3 week-old tobacco seedlings
530 grown in a controlled environment chamber at 130 µmol mol⁻² s⁻¹ and ambient (400 µmol
531 mol⁻¹) CO₂. Chlorophyll fluorescence parameters were obtained using a chlorophyll

532 fluorescence (CF) imaging system (Technologica, Colchester, UK^{49,50}). The operating
533 efficiency of photosystem two (PSII) photochemistry, F_q'/F_m' , was calculated from
534 measurements of steady state fluorescence in the light (F') and maximum fluorescence (F_m')
535 following a saturating 800 ms pulse of $6300 \mu\text{mol m}^{-2} \text{s}^{-1}$ PPFD and using the following
536 equation $F_q'/F_m' = (F_m' - F')/F_m'$. Images of F_q'/F_m' were taken under stable PPFD of 600
537 $\mu\text{mol m}^{-2} \text{s}^{-1}$ for Petite Havana and $650 \mu\text{mol m}^{-2} \text{s}^{-1}$ for Samsun⁵¹⁻⁵³.

538

539 **Leaf Gas Exchange**

540 Photosynthetic gas-exchange and chlorophyll fluorescence parameters were recorded
541 using a portable infrared gas analyser (LI-COR 6400; LI-COR, Lincoln, NE, USA) with a
542 6400-40 fluorometer head unit. Unless stated otherwise, all measurements were taken with
543 LI-COR 6400 cuvette. For plants grown in the glasshouse conditions were maintained at a
544 CO_2 concentration, leaf temperature and vapour pressure deficit (VPD) of $400 \mu\text{mol mol}^{-1}$, 25
545 $^\circ\text{C}$ and $1 \pm 0.2 \text{ kPa}$ respectively. The chamber conditions for plants grown under field
546 conditions had a CO_2 concentration of $400 \mu\text{mol mol}^{-1}$, block temperature was set to $2 \text{ }^\circ\text{C}$
547 above ambient temperature (ambient air temperature was measure before each curve) and
548 VPD was maintained as close to 1 kPa as feasible possible.

549

550 **A/C_i response curves (Photosynthetic capacity)**

551 The response of net photosynthesis (A) to intracellular CO_2 concentration (C_i) was
552 measured at a saturating light intensity of $2000 \mu\text{mol mol}^{-2} \text{s}^{-1}$. Illumination was provided by
553 a red-blue light source attached to the leaf cuvette. Measurements of A were started at
554 ambient CO_2 concentration (C_a) of $400 \mu\text{mol mol}^{-1}$, before C_a was decreased step-wise to a
555 lowest concentration of $50 \mu\text{mol mol}^{-1}$ and then increased step-wise to an upper concentration
556 of $2000 \mu\text{mol mol}^{-1}$. To calculate the maximum saturated CO_2 assimilation rate (A_{max}),

557 maximum carboxylation rate ($V_{C_{max}}$) and maximum electron transport flow (J_{max}), the C3
558 photosynthesis model⁵⁴ was fitted to the A/C_i data using a spreadsheet provided by Sharkey *et*
559 *al.*⁵⁵. Additionally, chlorophyll fluorescence parameters including PSII operating efficiency
560 (F_q'/F_m') and the coefficient of photochemical quenching (q_p), mathematically identical to
561 the PSII efficiency factor (F_q'/F_v') were recorded at each point.

562

563 ***A/Q* response curves**

564 Photosynthesis as a function of light (*A/Q* response curves) was measured under the
565 same cuvette conditions as the A/C_i curves mentioned above. Leaves were initially stabilized
566 at saturating irradiance of 2200 $\mu\text{mol m}^{-2} \text{s}^{-1}$, after which A and g_s were measured at the
567 following light levels: 2000, 1650, 1300, 1000, 750, 500, 400, 300, 200, 150, 100, 50 and 0
568 $\mu\text{mol m}^{-2} \text{s}^{-1}$). Measurements were recorded after A reached a new steady state (1-3 min) and
569 before g_s changed to the new light levels. Values of A and g_s were used to estimate intrinsic
570 water-use efficiency ($iWUE = A/g_s$)

571

572 **Monitoring electron transport and assimilation during light changes.**

573 A DUAL-PAM attached to a GFS-3000 (Walz, Effeltrich, Germany) was used to
574 monitor the response of the effective photochemical quantum yield of PSII (F_q'/F_m') and PSI
575 (Y(I)), and the net CO_2 Assimilation (A) to changes in light intensity. To remove stomatal
576 limitation of A , plants were maintained at constant temperature (24°C), relative humidity
577 (60%) and high $[\text{CO}_2]$ (1500 $\mu\text{mol mol}^{-1}$). Plants were dark adapted and the
578 induction/relaxation of the photosystems was tested by subjecting plants to a step change in
579 light intensity from 0 to 1000 $\mu\text{mol m}^{-2} \text{s}^{-1}$, this intensity was maintained for 5 min before
580 returning to dark.

581

582 **Statistical Analysis**

583 All statistical analyses were done using Sys-stat, University of Essex, UK, and R
584 (<https://www.r-project.org/>). For greenhouse and the 2016 field experiment biomass data,
585 seedling chlorophyll imaging and enzyme activities, analysis of variance and Post hoc Tukey
586 tests were done. For gas exchange curves, data were compared by linear mixed model
587 analysis using lmer function and type III anova⁵⁶. Significant differences between
588 manipulations were identified using contrasts analysis (lsmeans package). For the 2017 field
589 experiments, biomass data were compared by linear mixed model analysis using lmer
590 function and type III anova to account for block effect using four plants/genotype for n=6
591 blocks. For the analysis of electron transport and assimilation during light changes, the slope
592 of the activation curves was calculated for each parameter and analysis of variance and post-
593 hoc Tukey test was done.

594

595 **Data availability**

596 The data that support the findings of this study, plant transformation constructs and
597 seed are available from the corresponding authors on reasonable request.

598 **Figure Legends**

599

600 **Fig. 1. Screening of transgenic plants overexpressing FBP/SBPase, SBPase, and**
601 **cytochrome c_6 .**

602 (a) Immunoblot analysis of protein extracts from mature leaves of evaluated S_B , $S_B C_6$, S and
603 SC_6 lines compared to wild type and azygous (control, CN) plants, using FBP/SBPase and
604 SBPase antibodies. Equal amounts of protein were loaded, Transketolase (TK) is the loading
605 control. Repeated 3 times with similar results. (b) Immunoblot analysis of Cytochrome c_6
606 protein extract from mature leaves of C_6 compared to CN plants, ponceau staining was used
607 as loading control for plant samples only. Additionally, a crude *Porphyra sp.* protein extract is
608 presented as confirmation of correct band size for the introduced Cytochrome c_6 . Repeated 3
609 times with similar results (c) FBPase activity in S_B (n=16) and $S_B C_6$ (n=14) relative to CN
610 (n=6) plants. Chlorophyll fluorescence imaging of plants grown in controlled environmental
611 conditions was used to determine F_q'/F_m' (maximum PSII operating efficiency) at 600-650
612 $\mu\text{mol m}^{-2} \text{s}^{-1}$, 14 to 21 days after sowing (d) CN (n=20), S_B (n= 28), C_6 (n=29), $S_B C_6$ (n=30),
613 (e) CN (n=11), S (n=7) and SC_6 (n=6). Mean and SE is presented. Statistical tests used
614 analysis of variance and post-hoc Tukey test.

615

616 **Fig 2. Photosynthetic responses of transgenic plants grown in the glasshouse.**

617 Photosynthetic carbon fixation rates, operating efficiency of PSII in the light (F_q'/F_m'), PSII
618 efficiency factor (F_q'/F_v') and PSII maximum efficiency (F_v'/F_m') are presented in (a) mature
619 leaves CN (n=10), S_B (n=7), C_6 (n=11), $S_B C_6$ (n=9) cv. Petit Havana (b) mature leaves of CN
620 (n=10), S (n=8), SC_6 (n=10) and (c) developing leaves CN (n=6), S (n=6), SC_6 (n=9) cv.

621 Samsun. Parameters were determined as a function of increasing CO₂ concentrations at
622 saturating-light levels in developing (11-13cm in length) and mature leaves. Plants were
623 grown in the glasshouse where light levels oscillated between 400 and 1000 $\mu\text{mol m}^{-2} \text{s}^{-1}$
624 (supplemental light ensured a minimum of 400 $\mu\text{mol m}^{-2} \text{s}^{-1}$). Control group (CN) represent
625 both WT and azygous plants. Asterisks indicate significance between the transgenics and CN
626 plants, using a linear mixed-effects model and type III ANOVA and contrast analysis, *p <
627 0.05, exact p value indicated in each plot.

628

629 **Figure 3. Increased SBPase or expression of FBP/SBPase and cytochrome *c*₆ increases**
630 **biomass in glasshouse grown plants.**

631 Tobacco plants were germinated in growth cabinets and moved to the glasshouse at 10-14 d
632 post-germination. Forty-day-old (cv. Petit Havana) or fifty-six-day-old (cv. Samsun) plants
633 were harvested and plant height, leaf area and above-ground biomass (dry weight)
634 determined. Control group represent both WT and azygous plants (CN). cv. Petite Havana
635 CN (n=17), S_B (n=21), C₆ (n=18), (S_BC₆ n=18); cv. Samsun CN (n= 16), S (n=7, SC₆ (n=
636 13). Mean and SE is presented. Statistical analysis was ANOVA with post-hoc Tukey test.

637

638 **Figure 4. Simultaneous expression of FBP/SBPase and cytochrome *c*₆ increases biomass**
639 **in field grown plants.**

640 (a-c) Forty-day-old (young) 2016 field-grown plants (plants were germinated and grown in
641 glasshouse conditions for 26 d and then allowed to grow in the field in summer 2016 for 14
642 d); (d-i) Fifty-seven-day-old or sixty-one-day-old (flowering) 2017 field-grown plants (plants
643 were germinated and grown in glasshouse conditions for 26 d and grown in the field in
644 summer 2017 until flowering established, circa 30 d). Plant height, leaf area and total above-
645 ground biomass (dry weight) are shown. 2016 Experiment CN (n=72), S_B (n=33), C₆ (n=33);

646 2017 Experiment 1: CN (n=93), S_B (n=71), C₆ (n=70); 2017 Experiment 2: (n=97), C₆
647 (n=72), S_BC₆ (n=47) Mean ± SE presented. Statistical analysis was ANOVA with post-hoc
648 Tukey test.

649

650 **Fig 5. Photosynthetic capacity of field-grown transgenic plants.**

651 Photosynthetic carbon fixation rates and operating efficiency of PSII as a function of
652 increasing CO₂ concentrations at saturating-light levels in mature leaves from CN and
653 transgenic plants. (a) 2017 experiment 1: CN (n= 21), S_B (n=16) and C₆ (n=16). (b) 2017
654 experiment 2: Lines expressing cytochrome CN (n=22) C₆ (n=16), S_BC₆ (n=14). Control
655 group (CN) represent both WT and azygous plants. Mean ± SE presented. A linear mixed-
656 effects model and type III ANOVA was applied, exact p value indicated in each plot.

657

658 **Fig 6. Simultaneous expression of FBP/SBPase and cytochrome *c*₆ can increase water**
659 **use efficiency under field conditions.**

660 (a) Net CO₂ assimilation rate (*A*), (b) Stomatal conductance (*g*_s), (c) Intercellular CO₂
661 concentration (*C*_i), and (d) Intrinsic water-use efficiency (*iWUE*) as a function of light
662 (PPFD) in field-grown plants, CN n= 22, C₆ n=16, S_BC₆ n=14. A linear mixed-effects model
663 and type III ANOVA was applied, exact p value indicated in each plot.

664

665 **Table 1.** Maximum electron transport and RuBP regeneration rate (J_{max}), maximum
 666 carboxylation rate of Rubisco ($V_{c_{max}}$) and maximum assimilation (A_{max}) of WT and
 667 transgenic lines. Results were determined from the A/C_i curves in Figure 2 using the
 668 equations published by von Caemmerer and Farquhar⁵⁷. Significant differences are shown in
 669 boldface (* $p < 0.05$). cv. Samsun Mature leaves CN (n=10), S (n=8), SC₆ (n=10); developing
 670 leaves CN (n=6), S (n=6), SC₆ (n=9); cv. Petit Havana Mature leaves: CN (n=10), S_B (n=7),
 671 C₆ (n=11), S_BC₆ (n=9) Mean and SE are shown.
 672

		A/C_i		
Leaf Stage	Line	$V_{c_{max}}$ ($\mu\text{mol m}^{-2} \text{s}^{-1}$)	J_{max} ($\mu\text{mol m}^{-2} \text{s}^{-1}$)	A_{max} ($\mu\text{mol m}^{-2} \text{s}^{-1}$)
Developing	CN	72.32 ± 5.5	157.51 ± 6.0	29.6 ± 1.1
	S	87.7 ± 4.3	179.8 ± 4.9*	34.1 ± 0.7*
	SC ₆	86.5 ± 3.5	181.2 ± 3.6*	33.7 ± 1.1*
Samsun				
Mature	CN	77.2 ± 3.3	171.0 ± 6.0	31.6 ± 1.0
	S	81.3 ± 6.1	183.5 ± 9.0	32.2 ± 0.7
	SC ₆	90.3 ± 3.3	193.1 ± 5.4	34.9 ± 1.1*
Petit Havana	CN	69.6 ± 2.0	121.5 ± 1.3	24.6 ± 0.5
	S _B	69.0 ± 5.1	128.7 ± 3.8	27.0 ± 0.8
	C ₆	79.3 ± 7.0	129.9 ± 5.1	25.6 ± 0.5
	S _B C ₆	76.5 ± 4.2	132.0 ± 3.8	27.4 ± 0.8*

673

674

675 **References**

676

- 677 1 Zhu, X. G., Long, S. P. & Ort, D. R. Improving photosynthetic efficiency for greater
678 yield. *Annu Rev Plant Biol* **61**, 235-261, doi:10.1146/annurev-arplant-042809-112206
679 (2010).
- 680 2 Simkin, A. J., Lopez-Calcagno, P. E. & Raines, C. A. Feeding the world: Improving
681 photosynthetic efficiency for sustainable crop production. *Journal of Experimental*
682 *Botany*, doi:doi.org/10.1093/jxb/ery445 (2019).
- 683 3 Simkin, A. J. Genetic Engineering for Global Food Security: Photosynthesis and
684 Biofortification. *Plants* **8**, 586 (2019).
- 685 4 Miyagawa, Y., Tamoi, M. & Shigeoka, S. Overexpression of a cyanobacterial
686 fructose-1,6-/sedoheptulose-1,7-bisphosphatase in tobacco enhances photosynthesis
687 and growth. *Nat Biotechnol* **19**, 965-969, doi:10.1038/nbt1001-965 (2001).
- 688 5 Lefebvre, S. *et al.* Increased sedoheptulose-1,7-bisphosphatase activity in transgenic
689 tobacco plants stimulates photosynthesis and growth from an early stage in
690 development. *Plant physiology* **138**, 451-460, doi:10.1104/pp.104.055046 (2005).
- 691 6 Raines, C. A. Transgenic approaches to manipulate the environmental responses of
692 the C(3) carbon fixation cycle. *Plant Cell Environ* **29**, 331-339, doi:10.1111/j.1365-
693 3040.2005.01488.x (2006).
- 694 7 Rosenthal, D. M. *et al.* Over-expressing the C(3) photosynthesis cycle enzyme
695 Sedoheptulose-1-7 Bisphosphatase improves photosynthetic carbon gain and yield
696 under fully open air CO(2) fumigation (FACE). *BMC Plant Biol* **11**, 123,
697 doi:10.1186/1471-2229-11-123 (2011).
- 698 8 Simkin, A. J., McAusland, L., Headland, L. R., Lawson, T. & Raines, C. A.
699 Multigene manipulation of photosynthetic carbon assimilation increases CO₂ fixation
700 and biomass yield in tobacco. *J Exp Bot* **66**, 4075-4090, doi:10.1093/jxb/erv204
701 (2015).
- 702 9 Simkin, A. J. *et al.* Simultaneous stimulation of sedoheptulose 1,7-bisphosphatase,
703 fructose 1,6-bisphosphate aldolase and the photorespiratory glycine decarboxylase-H
704 protein increases CO₂ assimilation, vegetative biomass and seed yield in Arabidopsis.
705 *Plant Biotechnol J* **15**, 805-816, doi:10.1111/pbi.12676 (2017).
- 706 10 Zhu, X. G., de Sturler, E. & Long, S. P. Optimizing the distribution of resources
707 between enzymes of carbon metabolism can dramatically increase photosynthetic
708 rate: A numerical simulation using an evolutionary algorithm. *Plant physiology* **145**,
709 513-526, doi:DOI 10.1104/pp.107.103713 (2007).
- 710 11 Long, S. P., Zhu, X. G., Naidu, S. L. & Ort, D. R. Can improvement in photosynthesis
711 increase crop yields? *Plant Cell Environ* **29**, 315-330 (2006).
- 712 12 Poolman, M. G., Fell, D. A. & Thomas, S. Modelling photosynthesis and its control. *J*
713 *Exp Bot* **51**, 319-328, doi:DOI 10.1093/jexbot/51.suppl_1.319 (2000).
- 714 13 Raines, C. A. The Calvin cycle revisited. *Photosynth Res* **75**, 1-10, doi:Doi
715 10.1023/A:1022421515027 (2003).
- 716 14 Uematsu, K., Suzuki, N., Iwamae, T., Inui, M. & Yukawa, H. Increased fructose 1,6-
717 bisphosphate aldolase in plastids enhances growth and photosynthesis of tobacco
718 plants. *J Exp Bot* **63**, 3001-3009, doi:10.1093/jxb/ers004 (2012).
- 719 15 Ding, F., Wang, M. L., Zhang, S. X. & Ai, X. Z. Changes in SBPase activity
720 influence photosynthetic capacity, growth, and tolerance to chilling stress in
721 transgenic tomato plants. *Sci Rep-Uk* **6**, doi:ARTN 32741
722 10.1038/srep32741 (2016).

- 723 16 Driever, S. M. *et al.* Increased SBPase activity improves photosynthesis and grain
724 yield in wheat grown in greenhouse conditions. *Philosophical Transactions of the*
725 *Royal Society B* **372**, 1730 (2017).
- 726 17 Tamoi, M., Nagaoka, M., Miyagawa, Y. & Shigeoka, S. Contribution of fructose-1,6-
727 bisphosphatase and sedoheptulose-1,7-bisphosphatase to the photosynthetic rate and
728 carbon flow in the Calvin cycle in transgenic plants. *Plant Cell Physiology* **47**, 380-
729 390, doi:10.1093/pcp/pcj004 (2006).
- 730 18 Ichikawa, Y. *et al.* Generation of transplastomic lettuce with enhanced growth and
731 high yield. *GM Crops* **1**, 322-326, doi:10.4161/gmcr.1.5.14706 (2010).
- 732 19 Kohler, I. H. *et al.* Expression of cyanobacterial FBP/SBPase in soybean prevents
733 yield depression under future climate conditions. *J Exp Bot* **68**, 715-726,
734 doi:10.1093/jxb/erw435 (2017).
- 735 20 Simkin, A. J., McAusland, L., Lawson, T. & Raines, C. A. Overexpression of the
736 RieskeFeS Protein Increases Electron Transport Rates and Biomass Yield. *Plant*
737 *Physiol* **175**, 134-145, doi:10.1104/pp.17.00622 (2017).
- 738 21 Ermakova, M., Lopez-Calcagno, P. E., Raines, C. A., Furbank, R. T. & von
739 Caemmerer, S. Overexpression of the Rieske FeS protein of the Cytochrome *b₆*
740 complex increases C4 photosynthesis in *Setaria viridis*. *Communications Biology* **2**,
741 314, doi:10.1038/s42003-019-0561-9 (2019).
- 742 22 Chida, H. *et al.* Expression of the algal cytochrome *c₆* gene in Arabidopsis enhances
743 photosynthesis and growth. *Plant & cell physiology* **48**, 948-957,
744 doi:10.1093/pcp/pcm064 (2007).
- 745 23 Yadav, S. K., Khatri, K., Rathore, M. S. & Jha, B. Introgression of UfCyt *c₆*, a
746 thylakoid lumen protein from a green seaweed *Ulva fasciata* Delile enhanced
747 photosynthesis and growth in tobacco. *Molecular biology reports* **45(6)**, 1745-1758,
748 doi:10.1007/s11033-018-4318-1 (2018).
- 749 24 Merchant, S. & Bogorad, L. The Cu(II)-repressible plastidic cytochrome *c*. Cloning
750 and sequence of a complementary DNA for the pre-apoprotein. *Journal of Biological*
751 *Chemistry* **262**, 9062-9067 (1987).
- 752 25 De la Rosa M.A., M.-H. F. P., Hervás M., Navarro J.A. Convergent Evolution of
753 Cytochrome *c₆* and Plastocyanin. In: *Golbeck J.H. (eds) Photosystem I. Advances in*
754 *Photosynthesis and Respiration, vol 24. Springer, Dordrecht* (2006).
- 755 26 Finazzi, G., Sommer, F. & Hippler, M. Release of oxidized plastocyanin from
756 photosystem I limits electron transfer between photosystem I and cytochrome *b₆f*
757 complex in vivo. *Proc Natl Acad Sci U S A* **102**, 7031-7036,
758 doi:10.1073/pnas.0406288102 (2005).
- 759 27 Gong, H. Y. *et al.* Transgenic Rice Expressing Ictb and FBP/Sbpase Derived from
760 Cyanobacteria Exhibits Enhanced Photosynthesis and Mesophyll Conductance to
761 CO₂. *Plos One* **10**, doi:ARTN e0140928
762 10.1371/journal.pone.0140928 (2015).
- 763 28 Yadav, S. K., Khatri, K., Rathore, M. S. & Jha, B. Introgression of UfCyt *c₆*, a
764 thylakoid lumen protein from a green seaweed *Ulva fasciata* Delile enhanced
765 photosynthesis and growth in tobacco. *Mol Biol Rep*, doi:10.1007/s11033-018-4318-1
766 (2018).
- 767 29 Wullschleger, S. D. Biochemical Limitations to Carbon Assimilation in C(3) Plants -
768 a Retrospective Analysis of the A/Ci Curves from 109 Species. *J Exp Bot* **44**, 907-
769 920, doi:DOI 10.1093/jxb/44.5.907 (1993).
- 770 30 Pesaresi, P. *et al.* Mutants, Overexpressors, and Interactors of Arabidopsis
771 Plastocyanin Isoforms: Revised Roles of Plastocyanin in Photosynthetic Electron

- 772 Flow and Thylakoid Redox State. *Mol Plant* **2**, 236-248, doi:10.1093/mp/ssn041
773 (2009).
- 774 31 López-Calcagno, P. E. *et al.* Overexpressing the H₂O₂ protein of the glycine cleavage
775 system increases biomass yield in glasshouse and field-grown transgenic tobacco
776 plants. *Plant biotechnology journal* **17**, 141-151, doi:doi.org/10.1111/pbi.12953
777 (2018).
- 778 32 Glowacka, K. *et al.* Photosystem II Subunit S overexpression increases the efficiency
779 of water use in a field-grown crop. *Nat Commun* **9**, doi:ARTN 868
780 10.1038/s41467-018-03231-x (2018).
- 781 33 Busch, F. A. Opinion: The red-light response of stomatal movement is sensed by the
782 redox state of the photosynthetic electron transport chain. *Photosynth Res* **119**, 131-
783 140, doi:10.1007/s11120-013-9805-6 (2014).
- 784 34 Engler, C., Gruetzner, R., Kandzia, R. & Marillonnet, S. Golden Gate Shuffling: A
785 One-Pot DNA Shuffling Method Based on Type IIs Restriction Enzymes. *Plos One* **4**,
786 doi:ARTN e5553
787 10.1371/journal.pone.0005553 (2009).
- 788 35 Engler, C., Kandzia, R. & Marillonnet, S. A one pot, one step, precision cloning
789 method with high throughput capability. *Plos One* **3**, e3647,
790 doi:10.1371/journal.pone.0003647 (2008).
- 791 36 Nakagawa, T. *et al.* Development of series of gateway binary vectors, pGWBs, for
792 realizing efficient construction of fusion genes for plant transformation. *Journal of*
793 *bioscience and bioengineering* **104**, 34-41, doi:10.1263/jbb.104.34 (2007).
- 794 37 Simkin, A. J. *et al.* Characterization of the plastidial geraniol synthase from
795 *Madagascar periwinkle* which initiates the monoterpenoid branch of the alkaloid
796 pathway in internal phloem associated parenchyma. *Phytochemistry* **85**, 36-43,
797 doi:10.1016/j.phytochem.2012.09.014 (2013).
- 798 38 Richins, R. D., Scholthof, H. B. & Shepherd, R. J. Sequence of Figwort Mosaic-Virus
799 DNA (Caulimovirus Group). *Nucleic acids research* **15**, 8451-8466, doi:DOI
800 10.1093/nar/15.20.8451 (1987).
- 801 39 Horsch, R. B., Rogers, S. G. & Fraley, R. T. Transgenic Plants - Technology and
802 Applications. *Abstr Pap Am Chem S* **190**, 67 (1985).
- 803 40 Hoagland, D. R. & Arnon, D. I. *The water-culture method for growing plants without*
804 *soil*. (The College of Agriculture, 1950).
- 805 41 Kromdijk, J. *et al.* Improving photosynthesis and crop productivity by accelerating
806 recovery from photoprotection. *Science* **354**, 857-861, doi:10.1126/science.aai8878
807 (2016).
- 808 42 Lopez-Calcagno, P. E., Abuzaid, A. O., Lawson, T. & Raines, C. A. Arabidopsis
809 CP12 mutants have reduced levels of phosphoribulokinase and impaired function of
810 the Calvin-Benson cycle. *J Exp Bot* **68**, 2285-2298, doi:10.1093/jxb/erx084 (2017).
- 811 43 Dunford, R. P., Catley, M. A., Raines, C. A., Lloyd, J. C. & Dyer, T. A. Purification
812 of active chloroplast sedoheptulose-1,7-bisphosphatase expressed in *Escherichia coli*.
813 *Protein expression and purification* **14**, 139-145, doi:10.1006/pep.1998.0939 (1998).
- 814 44 Henkes, S., Sonnewald, U., Badur, R., Flachmann, R. & Stitt, M. A small decrease of
815 plastid transketolase activity in antisense tobacco transformants has dramatic effects
816 on photosynthesis and phenylpropanoid metabolism. *The Plant cell* **13**, 535-551
817 (2001).
- 818 45 Khozaei, M. *et al.* Overexpression of plastid transketolase in tobacco results in a
819 thiamine auxotrophic phenotype. *The Plant cell* **27**, 432-447,
820 doi:10.1105/tpc.114.131011 (2015).

- 821 46 Timm, S. *et al.* Glycine decarboxylase controls photosynthesis and plant growth.
822 *FEBS letters* **586**, 3692-3697, doi:10.1016/j.febslet.2012.08.027 (2012).
- 823 47 Hiyama, T. Isolation of photosystem I particles from spinach. *Methods Mol Biol* **274**,
824 11-17, doi:10.1385/1-59259-799-8:011 (2004).
- 825 48 Zhao, Y. L. *et al.* Downregulation of Transketolase Activity Is Related to Inhibition
826 of Hippocampal Progenitor Cell Proliferation Induced by Thiamine Deficiency.
827 *Biomed Res Int*, doi:Artn 572915
828 10.1155/2014/572915 (2014).
- 829 49 Barbagallo, R. P., Oxborough, K., Pallett, K. E. & Baker, N. R. Rapid, noninvasive
830 screening for perturbations of metabolism and plant growth using chlorophyll
831 fluorescence imaging. *Plant physiology* **132**, 485-493, doi:10.1104/pp.102.018093
832 (2003).
- 833 50 von Caemmerer, S. *et al.* Stomatal conductance does not correlate with photosynthetic
834 capacity in transgenic tobacco with reduced amounts of Rubisco. *J Exp Bot* **55**, 1157-
835 1166, doi:10.1093/jxb/erh128 (2004).
- 836 51 Baker, N. R., Oxborough, K., Lawson, T. & Morison, J. I. L. High resolution imaging
837 of photosynthetic activities of tissues, cells and chloroplasts in leaves. *Journal of*
838 *Experimental Botany* **52**, 615-621 (2001).
- 839 52 Oxborough, K. & Baker, N. R. An evaluation of the potential triggers of
840 photoinactivation of photosystem II in the context of a Stern–Volmer model for
841 downregulation and the reversible radical pair equilibrium model. *Philosophical*
842 *Transactions of the Royal Society of London. Series B: Biological Sciences* **355**, 1489-
843 1498 (2000).
- 844 53 Lawson, T., Lefebvre, S., Baker, N. R., Morison, J. I. L. & Raines, C. A. Reductions
845 in mesophyll and guard cell photosynthesis impact on the control of stomatal
846 responses to light and CO₂. *J Exp Bot* **59**, 3609-3619, doi:10.1093/jxb/ern211
847 (2008).
- 848 54 Farquhar, G., von Caemmerer, S. v. & Berry, J. A biochemical model of
849 photosynthetic CO₂ assimilation in leaves of C₃ species. *Planta* **149**, 78-90 (1980).
- 850 55 Sharkey, T. D., Bernacchi, C. J., Farquhar, G. D. & Singsaas, E. L. Fitting
851 photosynthetic carbon dioxide response curves for C₃ leaves. *Plant Cell Environ* **30**,
852 1035-1040, doi:10.1111/j.1365-3040.2007.01710.x (2007).
- 853 56 Vialet-Chabrand, S., Matthews, J. S. A., Simkin, A. J., Raines, C. A. & Lawson, T.
854 Importance of Fluctuations in Light on Plant Photosynthetic Acclimation. *Plant*
855 *physiology* **173**, 2163-2179, doi:10.1104/pp.16.01767 (2017).
- 856 57 von Caemmerer, S. & Farquhar, G. D. Some Relationships between the Biochemistry
857 of Photosynthesis and the Gas-Exchange of Leaves. *Planta* **153**, 376-387, doi:Doi
858 10.1007/Bf00384257 (1981).
- 859

860 **Acknowledgments**

861 This study was supported by the Realising Improved Photosynthetic Efficiency
862 (RIPE) initiative awarded to C.A.R by University of Illinois, USA. RIPE was possible
863 through support from the Bill & Melinda Gates Foundation, DFID and FFAR, grant
864 OPP1172157. This work was also supported by the Biotechnology and Biological Sciences
865 Research Council (BBSRC) grant BB/J004138/1. We would like to thank Jack Matthews
866 (University of Essex) for help with data analysis, Elena A. Pelech (University of Illinois) and
867 Sunitha Subramaniam (University of Essex) for help with plant growth, Phillip A. Davey
868 (University of Essex) and Richard Gossen (University of Helsinki) for help with gas
869 exchange and David Drag, Ben Harbaugh and the Ort lab (University of Illinois) for support
870 with the field trials.

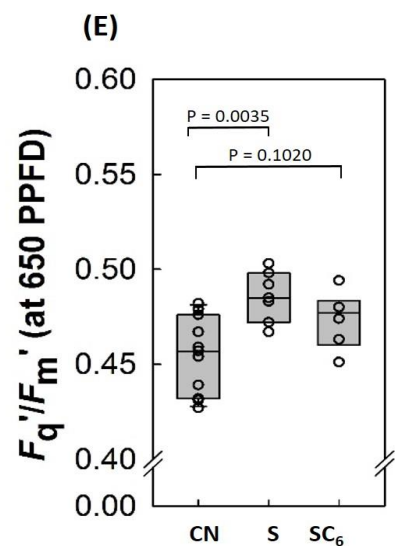
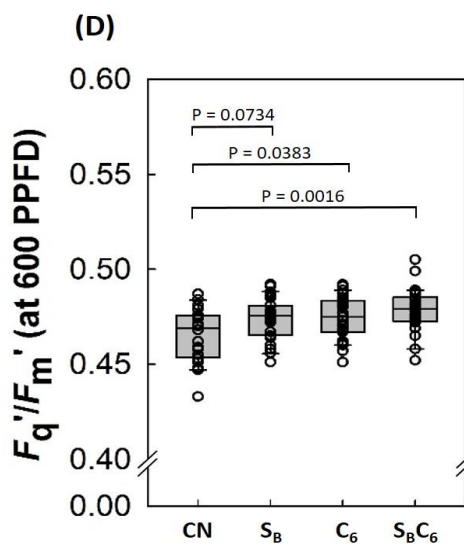
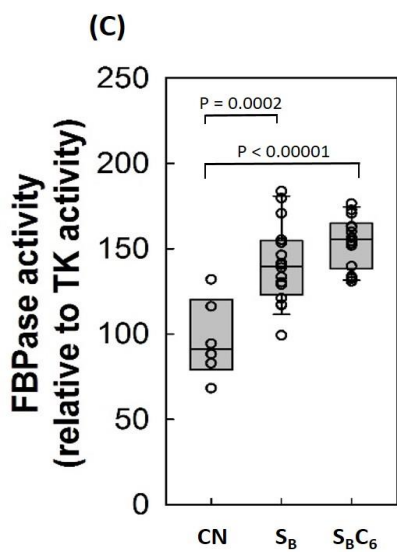
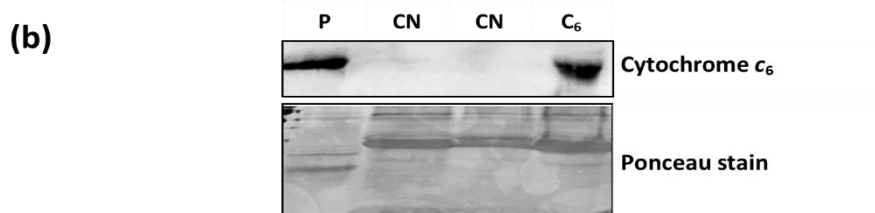
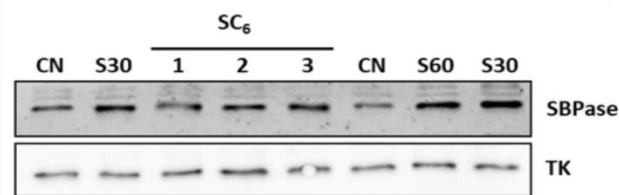
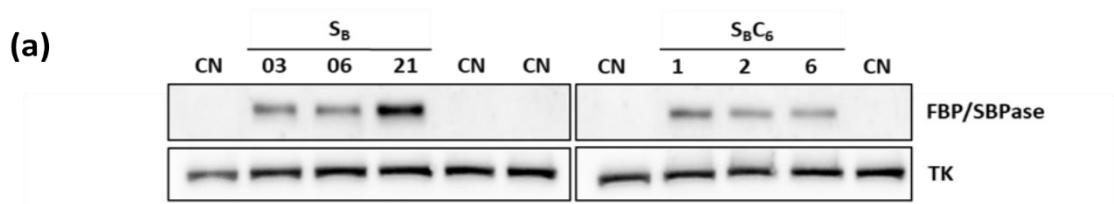
871

872 **Author contributions**

873 P.E.L.C and A.J.S. generated transgenic plants. P.E.L.C, A.J.S, K.L.B. and S.J.F. performed
874 molecular and biochemical experiments. P.E.L.C, A.J.S and K.L.B carried out plant
875 phenotypic and growth analysis and performed gas exchange measurement, S.V.C. made the
876 measurements of photosynthesis during light induction. A.J.S and S.J.F performed enzyme
877 assays on selected lines; all authors carried out data analysis on their respective contributions;
878 C.A.R and T.L designed and supervised the research; P.E.L.C., A.J.S and C.A.R wrote the
879 manuscript, TL contributed to editing of the manuscript and finalising of figures. P.E.L.C,
880 K.L.B. and A.J.S contributed equally to the completion of this work.

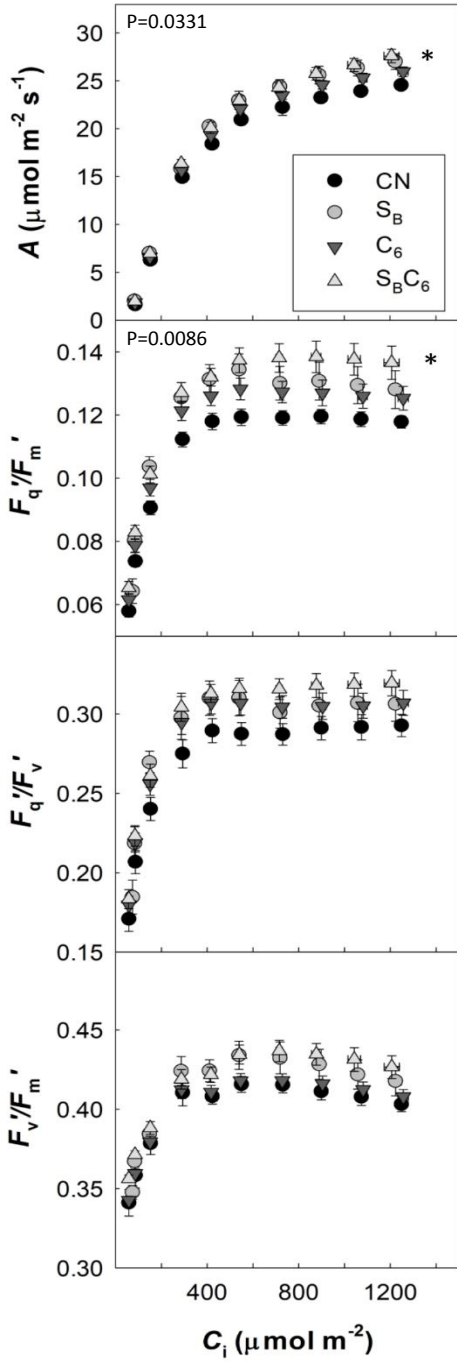
881

882 **Competing interests:** The authors declare no competing financial interests



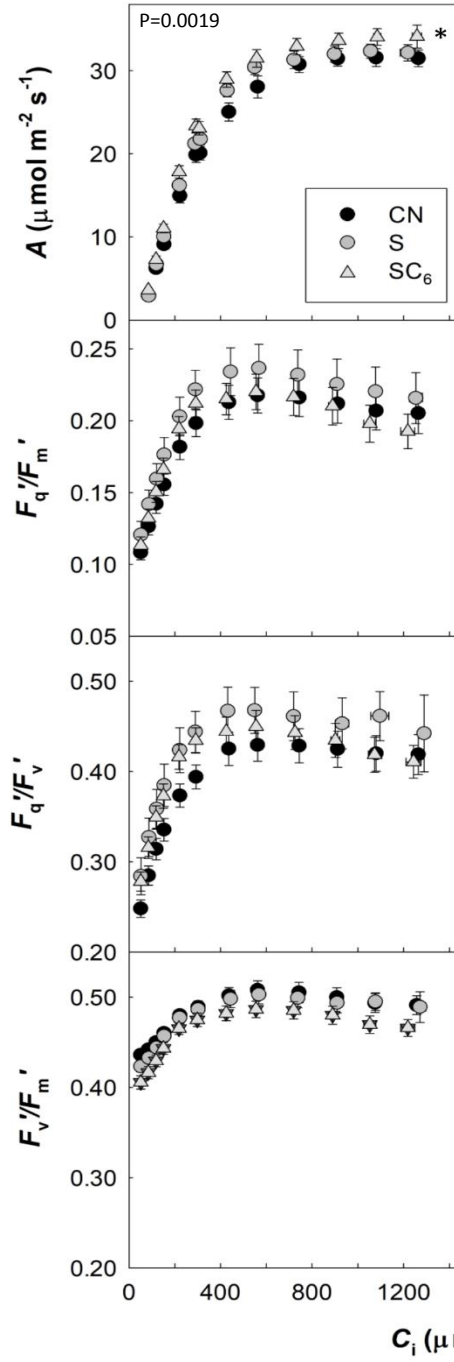
cv. Petite Havana

(a) Mature leaf

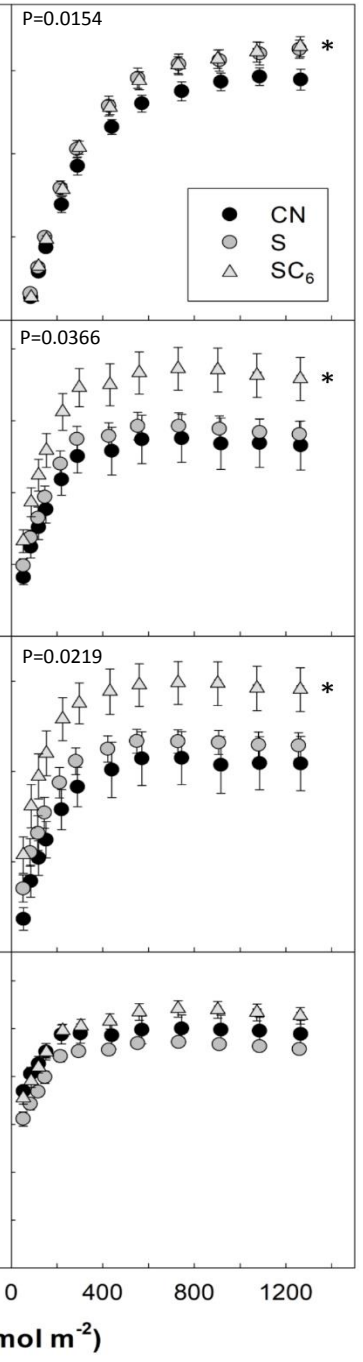


cv. Samsun

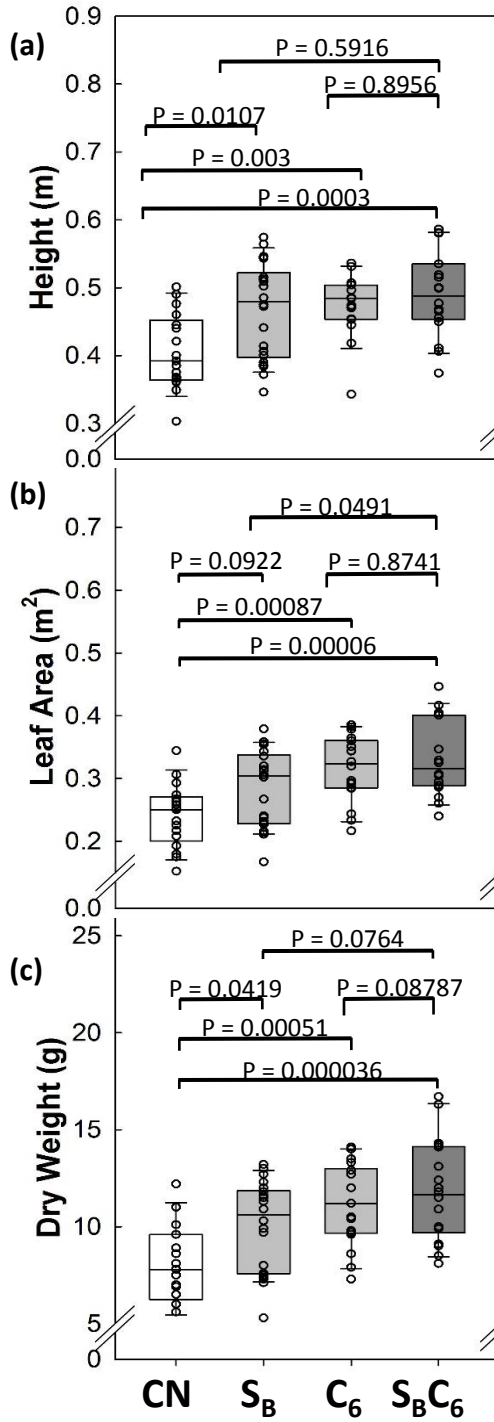
(b) Mature leaf



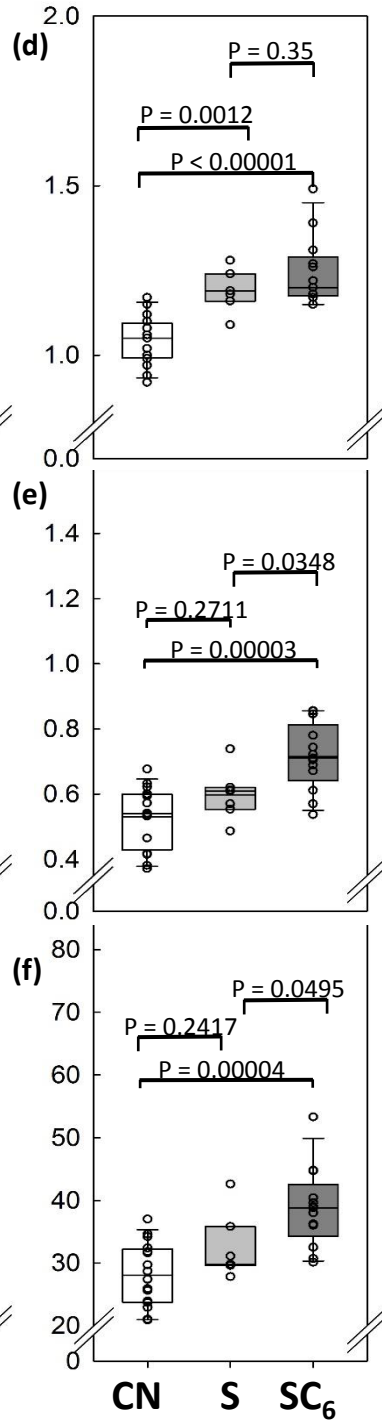
(c) Developing leaf

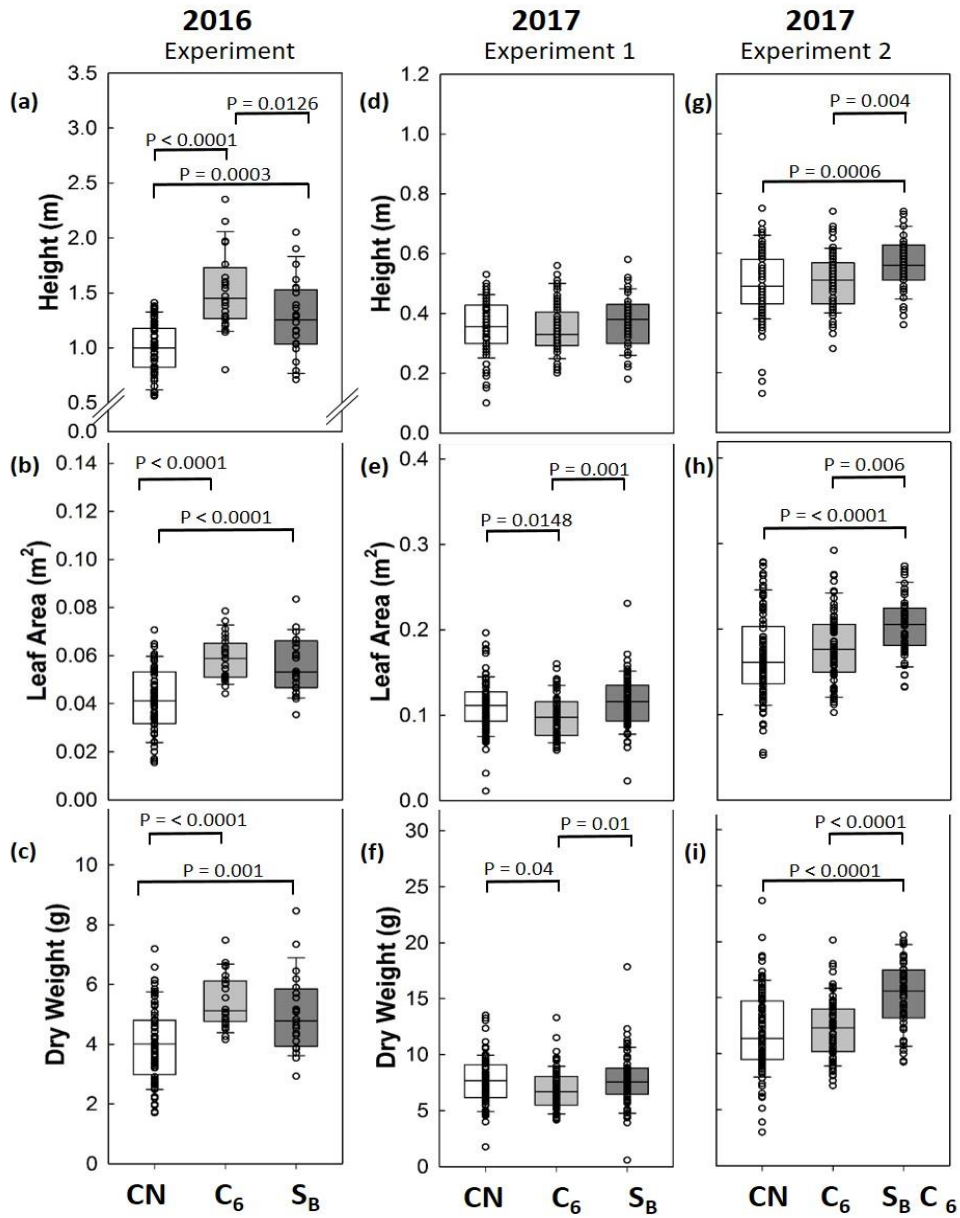


cv. Petite Havana



cv. Samsun

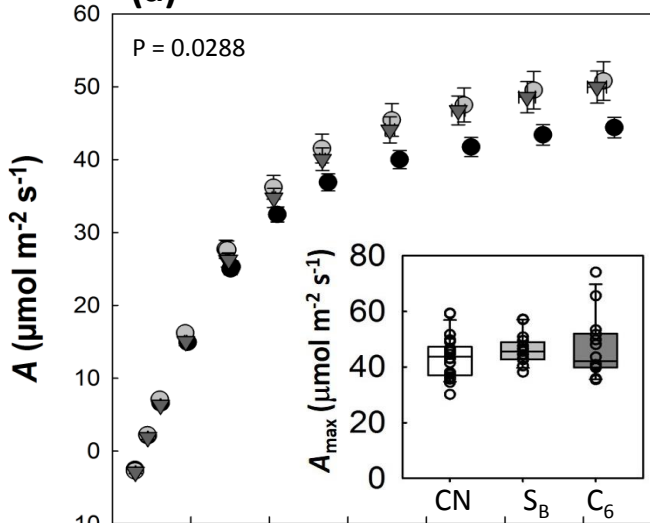




2017

Experiment 1

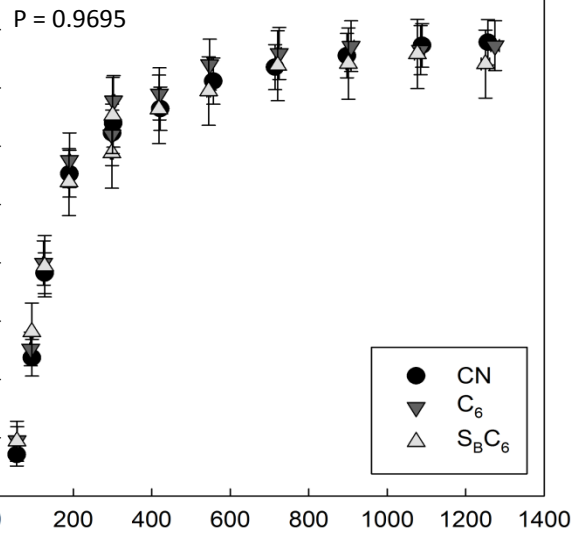
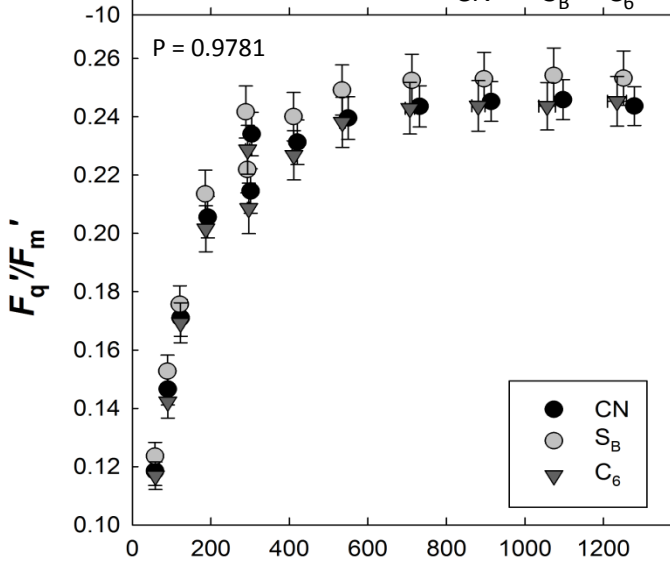
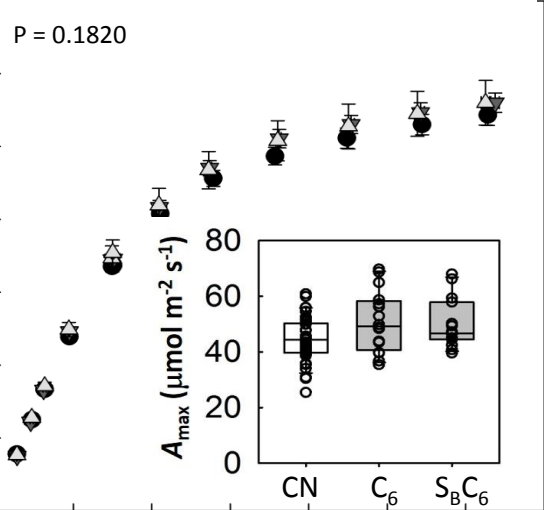
(a)



2017

Experiment 2

(b)



C_i ($\mu\text{mol m}^{-2}$)

2017
Experiment 2

